

# Swinging Up and Stabilization of a Real Inverted Pendulum

Nenad Muškinja, *Member, IEEE*, and Boris Tovornik, *Member, IEEE*

**Abstract**—The basic aim of the present work was to swing up a real pendulum from the pending position and to balance stably the pendulum at the upright position and further move the pendulum cart to a specified position on the pendulum rail in the shortest time. Different control strategies are compared and tested in simulations and in real-time experiments, where maximum acceleration of the pendulum pivot and length of the pendulum rail are limited. A comparison of fuzzy swinging algorithm with energy-based swinging strategies shows advantages of using fuzzy control theory in nonlinear real-time applications. An adaptive state controller was developed for a stabile, and in the same time optimal balancing of an inverted pendulum and a switching mechanism between swinging and balancing algorithm is proposed.

**Index Terms**—Adaptive control, cart-pendulum system, fuzzy control, nonlinear control systems, stabilization, swing up.

## I. INTRODUCTION

CONTROLLING the inverted pendulum is a classic experiment that is used in control laboratories. Because of its nonlinear nature, the pendulum is now used to illustrate many of the ideas emerging in the field of nonlinear control. There are several tasks to be solved, such as swinging up and catching the pendulum from its stable pending position to the upright unstable position, and then balancing the pendulum at the upright position during disturbances, and further move the cart to a specified position of the cart on the rail. Many approaches for swinging and catching of an inverted pendulum have been proposed in the literature; from Furuta *et al.* [1] with minimum time controller, which is unfortunately not very robust, to Åström and Furuta [2] with energy control strategy, which controls the energy of the inverted pendulum toward a value equal to the steady-state upright position, and Yi *et al.* [3] with a fuzzy controller based on single input rule modules. There have been several fuzzy-model-based approaches concerning the stability of such nonlinear systems. Yurkovich and Widjaja [4] fully analyzed the control-engineering design procedures for an implementation of fuzzy-system concepts, and extend the linear quadratic fuzzy-based controller design to adapt to the changing system parameters in balancing control for the rotational inverted pendulum. Leung *et al.* [5] introduced a simple parallel distributed compensation (PDC) design technique for Takagi–Sugeno fuzzy logic controller (FLC) that can

guarantee a closed-loop stability. Wang *et al.* [6] also presented a design methodology for stabilization of a class of nonlinear systems based on Takagi–Sugeno fuzzy model and PDC control design, where stability analysis and control-design problems are reduced to linear matrix inequality problems. Both solutions have been successfully applied in simulations on a cart inverted-pendulum model.

While controlling a real inverted pendulum, we are faced up with several limitations and constraints that were not considered in those approaches. Instead of driving the cart force (acceleration) directly, in particular case, the cart velocity is driven over dc-motor voltage, so we must consider the cart-velocity limitations instead of the cart-acceleration limitations. Another very important limitation is that the rail has a limited length and, thus, the cart movement is limited. In the literature, there are several solutions for swing up and stabilization of a cart pendulum with a restricted travel. Wei *et al.* [7] presented a nonlinear control strategy by decomposing the control law into a sequence of steps. Chung and Hauser [8] proposed a nonlinear state controller that controls the cart position and the swinging energy of the pendulum at the same time. Lin and Sheu [9] proposed a hybrid-control approach that combines a FLC and a linear state feedback controller that stabilizes the linearized model of the inverted pendulum having a restricted travel. Zhao and Spong [10] applied a hybrid-control strategy, which globally asymptotically stabilizes the system for all initial conditions. Chatterjee *et al.* [11] proposed an energy-based control law that swings up and stabilizes a cart-pendulum system with restricted travel and restricted control force in simulations as well as in real-time experiments.

In this paper, a new fuzzy swinging algorithm is proposed and compared with energy-based strategy, which is derived from the exact nonlinear mathematical model of the inverted pendulum. While swinging up the pendulum with simple fuzzy controller, the energy of the pendulum is driven toward a value equal to the steady-state upright position. The pendulum then approaches the upright position where it can be caught with an appropriate strategy. The problem is to stabilize the pendulum at the upper steady-state position and to stop the movement of the cart at the desired position of the cart on the rail. The state-controller parameter adaptation solves this problem and also improves the stability of the closed-loop system. For this purpose, exact mathematical model of the real inverted pendulum has been derived and linearized at the upright steady-state position. All experiments have been done in simulations on the nonlinear mathematical model of the inverted pendulum and in real-time experiments on the real inverted-pendulum system.

Manuscript received March 12, 2004; revised June 10, 2005. Abstract published on the Internet January 25, 2006.

The authors are with the Faculty of Electrical Engineering and Computer Science, University of Maribor, Maribor 2000, Slovenia (e-mail: nenad.muskinja@uni-mb.si).

Digital Object Identifier 10.1109/TIE.2006.870667

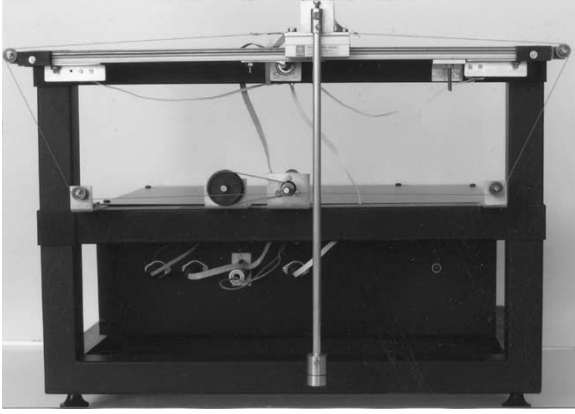


Fig. 1. Inverted-pendulum construction.

## II. REAL INVERTED-PENDULUM SYSTEM

The real inverted-pendulum system (Fig. 1) considered here consists of the cart that is moving on a rail and the pole that is mounted on the cart via the pole shaft so that it can swing freely in the vertical plane. The translation of the cart is enabled by the dc motor. The shaft of the motor is connected with the cart by a thin steel wire. Control algorithm and data acquisition and visualization were realized with MathWorks Matlab, Simulink, and Real-Time xPC target products on a personal computer with the 12-bit AD/DA converter.

Because of the limited pendulum-rail length (0.5 m), the pendulum-cart movement is also limited ( $\pm 0.25$  m).

## III. MODELING OF AN INVERTED PENDULUM

The model of the inverted-pendulum system can be divided into three separate models: the inverted-pendulum model (the mechanical system of the cart and the pole), the dc-motor model, and the transmission model.

### A. Inverted Pendulum and Cart Model

Modeling of an inverted pendulum with respect to the Lagrange equations gives

$$F - F_{fr} = a\ddot{x} + b\ddot{\varphi} \cos \varphi - b\dot{\varphi}^2 \sin \varphi \quad (1)$$

and

$$M - M_{fr} = c\ddot{\varphi} + b\ddot{x} \cos \varphi - bg \sin \varphi \quad (2)$$

where

$$a = m_1 + m_2 + m_T + \frac{J_{px}}{R_{px}^2} + \frac{J_p}{R^2} \quad (3)$$

$$b = m_2 L + m_T L_T \quad (4)$$

and

$$c = m_2 L^2 + m_T L_T^2 + J_T. \quad (5)$$

$F$  is an external force that moves the cart in the horizontal plane,  $F_{fr}$  is a cart friction,  $M$  is an external pole moment,  $M_{fr}$

is a pole friction moment,  $x$ ,  $\dot{x}$ , and  $\ddot{x}$  are cart position, cart velocity, and cart acceleration, respectively, and  $\varphi$ ,  $\dot{\varphi}$ , and  $\ddot{\varphi}$  are pole angle, angle velocity, and angle acceleration, respectively.

*Model Constant Determination:*

$g$  Acceleration due gravity:  $g = 9.81 \text{ m/s}^2$ .

$m_1$  Common cart mass:  $m_1 = 0.128 \text{ kg}$ .

$m_2$  Mass of the weight:  $m_2 = 0.063 \text{ kg}$ .

$m_T$  Pole mass:  $m_T = 0.043 \text{ kg}$ .

$L$  Distance from the pivot to the center of the weight mass at the top of the pole  $m_2$ :  $L = 0.33 \text{ m}$ .

$L_T$  Distance from the pivot to the center of the pole mass:  $L_T = 0.17 \text{ m}$ .

$J_T$  Moment of inertia of the pole with respect to the pivot point:  $J_T = 4.14 \times 10^{-4} \text{ kg} \cdot \text{m}^2$ .

$R$  Radius of the dc-motor shaft:  $R = 0.003 \text{ m}$ .

$R_{px}$  Radius of the belt wheel for cart-position measuring.

$J_{px}$  Moment of inertia of the belt wheel:  $J_{px} = 1.22 \times 10^{-6} \text{ kg} \cdot \text{m}^2$ .

$J_p$  Moment of inertia of the dc-motor shaft:  $J_p = 3.33 \times 10^{-7} \text{ kg} \cdot \text{m}^2$ .

### B. DC-Motor Model

$$u_a = L_a \dot{i}_a + R_a i_a + K_e \omega \quad (6)$$

$$M_{el} = K_m i_a \quad (7)$$

and

$$M_{el} - M_b = J_m \dot{\omega} + B_m \omega \quad (8)$$

where  $u_a$  is a motor voltage,  $i_a$  is a motor coil current,  $R_a$  is a real motor coil resistance,  $L_a$  is a motor coil inductivity,  $K_e$  is a motor inductive constant,  $K_m$  is a motor moment constant,  $J_m$  is a motor rotor moment of inertia,  $B_m$  is a motor viscosity friction constant,  $\omega$  is a motor angle velocity,  $M_{el}$  is a motor electrical moment, and  $M_b$  is a motor load moment. Values of constants are:  $R_a = 2.7 \Omega$ ,  $L_a = 300 \mu\text{H}$ ,  $K_e = 0.0201 \text{ V} \cdot \text{s/rad}$ ,  $K_m = 0.02 \text{ N} \cdot \text{m/A}$ ,  $B_m = 1.1 \times 10^{-6} \text{ N} \cdot \text{m} \cdot \text{s/rad}$ , and  $J_m = 18 \times 10^{-7} \text{ kg} \cdot \text{m}^2$ .

### C. Transmission Model

$$\omega = \frac{G}{R_1} \dot{x} \quad (9)$$

and

$$M_b = \frac{R}{G} F \quad (10)$$

where  $R_1$  is the radius of the dc-motor shaft added with half of the diameter of the steely yarn. It must be exactly measured.  $R_1 = 0.0031 \text{ m}$  and  $G$  is the transmission reduction

$$G = \frac{R}{R_R} = \frac{\omega}{\omega_R} \doteq 1. \quad (11)$$

#### D. Common Inverted-Pendulum Model

$$u_a = L_a \dot{i}_a + R_a i_a + K_e \frac{G}{R} \dot{x} \quad (12)$$

$$M_{el} = K_m i_a \quad (13)$$

$$M_{el} = a_1 \frac{G}{R} \ddot{x} + B_m \frac{G}{R} \dot{x} + b_1 \ddot{\varphi} \cos \varphi - b_1 \dot{\varphi}^2 \sin \varphi + \frac{R}{G} F_{tr} \quad (14)$$

and

$$M_{el} = \left( b_1 \cos \varphi - \frac{a_1 c}{b_1 \cos \varphi} \right) \ddot{\varphi} - b_1 \dot{\varphi}^2 \sin \varphi + c_1 \tan \varphi + B_m \frac{G}{R} \dot{x} + \frac{a_1}{b_1 \cos \varphi} (M - M_{tr}) + \frac{R}{G} F_{tr} \quad (15)$$

with

$$a_1 = J_m + \frac{aR^2}{G^2} \quad (16)$$

$$b_1 = \frac{bR}{G} \quad (17)$$

and

$$c_1 = a_1 \frac{gG}{R} \quad (18)$$

where  $a_1 = 5.1627 \times 10^{-6} \text{ kg} \cdot \text{m}^2$ ,  $b_1 = 8.7110 \times 10^{-5} \text{ kg} \cdot \text{m}^2$ , and  $c_1 = 0.0163 \text{ N} \cdot \text{m}$ .

#### E. Common Linear State Space Model

Common linear state space model is derived for small pole angles  $\varphi \cong 0$  and with negligible pendulum frictions  $F_{fr} = M_{fr} = 0$ .

$$\begin{aligned} \dot{\mathbf{x}} &= \mathbf{A}\mathbf{x} + \mathbf{B}u_a \\ \mathbf{y} &= \mathbf{C}\mathbf{x} + \mathbf{D}u_a \end{aligned} \quad (19)$$

where

$$\begin{aligned} \mathbf{A} &= \begin{bmatrix} 0 & 1 & 0 & 0 \\ 0 & -\frac{K_m K_e}{a_1 R} \left( 1 + \frac{b_1}{d_1} \right) & -\frac{R b_1 c_1}{G a_1 d_1} & 0 \\ 0 & 0 & 0 & 1 \\ 0 & \frac{K_m K_e G}{d_1 R a} & \frac{c_1}{d_1} & 0 \end{bmatrix} \\ &= \begin{bmatrix} 0 & 1 & 0 & 0 \\ 0 & -33.746 & -2.1107 & 0 \\ 0 & 0 & 0 & 1 \\ 0 & 111.33 & 39.327 & 0 \end{bmatrix} \\ \mathbf{B} &= \begin{bmatrix} 0 \\ \frac{R K_m}{G a_1 R a} \left( 1 + \frac{b_1}{d_1} \right) \\ 0 \\ -\frac{K_m}{d_1 R a} \end{bmatrix} = \begin{bmatrix} 0 \\ 5.3725 \\ 0 \\ -17.724 \end{bmatrix} \\ \mathbf{C} &= \begin{bmatrix} 1 & 0 & 0 & 0 \\ 0 & 0 & 1 & 0 \end{bmatrix} \\ \mathbf{D} &= \begin{bmatrix} 0 \\ 0 \end{bmatrix} \\ \mathbf{x}^T &= [x \quad \dot{x} \quad \varphi \quad \dot{\varphi}] \quad \text{and} \quad \mathbf{y}^T = [x \quad \varphi]. \end{aligned} \quad (20)$$

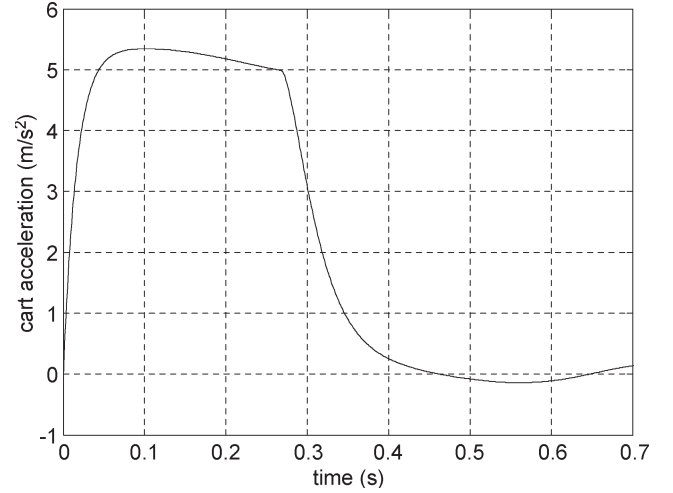


Fig. 2. Time response of the pendulum-cart acceleration applying a maximum voltage on a dc motor.

1) *Stability*: From  $\det(s\mathbf{I} - \mathbf{A}) = 0$  follows:  $s_1 = 0$ ,  $s_2 = -33.9570$ ,  $s_3 = 5.7777$ , and  $s_4 = -5.5667$ .

The linear model of the inverted pendulum is unstable.

2) *Controllability*: The rank of the controllability matrix is

$$\mathbf{Q}_C = [\mathbf{B} \quad \mathbf{AB} \quad \mathbf{A}^2\mathbf{B} \quad \mathbf{A}^3\mathbf{B}] \quad (21)$$

and  $\text{rank}(\mathbf{Q}_C) = 4$ , so the linear model of inverted pendulum is controllable.

#### IV. SWINGING UP A PENDULUM

Two different strategies have been considered: energy-based control purposed by Åström and Furuta [2] and extended by Chatterjee *et al.* [11] and a simple fuzzy-rule-based control.

##### A. Energy Control—Multiswing Behavior

The number of swings needed to swing up the pendulum from its pending position to its upright position critically depends on the ratio of the maximum acceleration of the pendulum pivot to the acceleration of gravity and, therefore, on the maximum acceleration of the pendulum cart. In the real inverted pendulum considered here, the maximum acceleration of the cart is to be estimated from simulations on the nonlinear mathematical model of the inverted pendulum derived in Section III.

Fig. 2 shows the time response of the pendulum-cart acceleration applying a maximum voltage on the dc motor  $u = u_{\max} = 10 \text{ V}$ .

The maximum acceleration of the pendulum cart is  $\ddot{x}_{\max} = 0.5345 \text{ [m/s}^2\text{]}$ , but only the effective value of the cart acceleration is to be considered, because we can control only the cart velocity and not the cart acceleration as Åström and Furuta [2] did in their work. The effective value of the pendulum-cart acceleration is generally

$$\ddot{x}_{\text{ef}} = \sqrt{\frac{1}{T} \int_0^T \ddot{x}^2(t) dt} \quad (22)$$

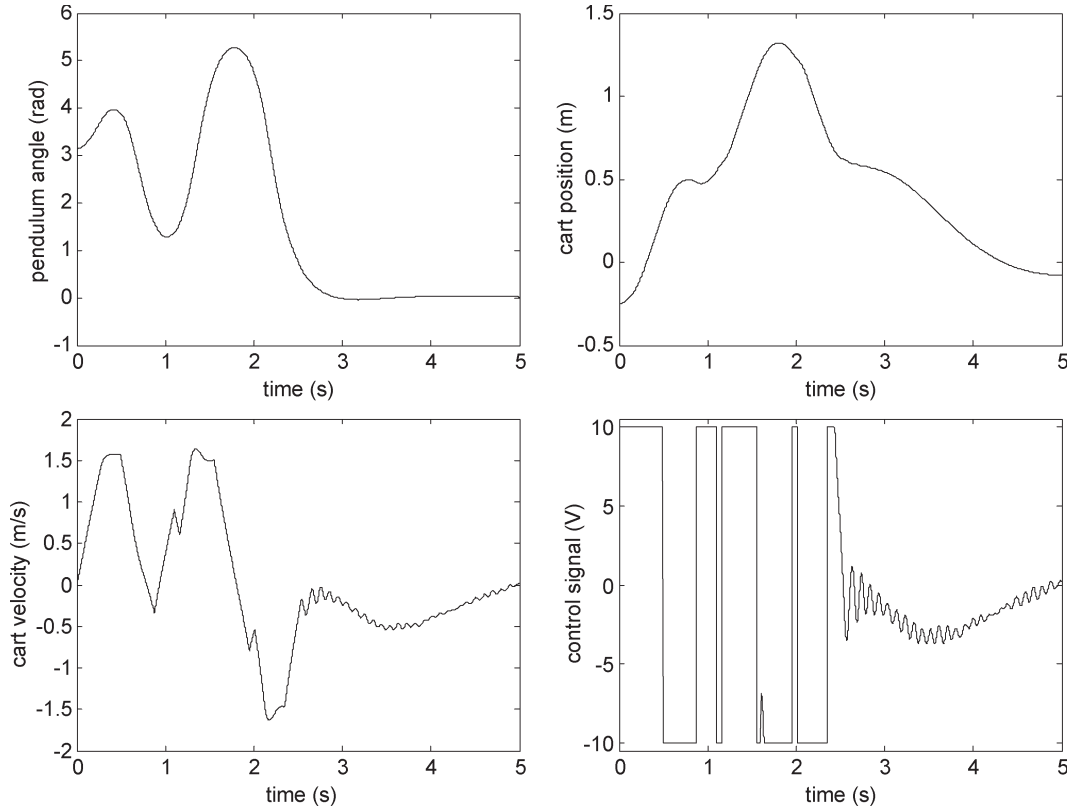


Fig. 3. Swinging up the pendulum with the energy control in four swings and stabilization with the state controller.

and it can be calculated numerically from the signal shown in Fig. 2. The effective value of the pendulum-cart acceleration that can be applied on the real inverted pendulum is then:  $\ddot{x}_{ef} = 3.5318 \text{ m/s}^2$ .

In general, the corresponding equation for the case of  $k$  swings is

$$2 \cdot \sin(\varphi_0) \geq 1 + \cos((2k-1)\varphi_0) \quad (23)$$

where  $2\varphi_0$  is a maximum angle of the pendulum reached after the first swing. Solving this equation numerically, we obtain the following relation between the acceleration of the pendulum cart and the number of swings  $k$ :

$n$	1.333	0.577	0.388	0.296	0.241	0.128
$k$	1	2	3	4	5	10

where  $n = \ddot{x}_{ef}/g$ , and  $g$  is an acceleration due the gravity, and, therefore

$$n = \frac{\ddot{x}_{ef}}{g} = \frac{3.5318}{9.81} = 0.342.$$

This means that at least four swings will be needed to swing up the real inverted pendulum considered here.

To apply the energy control algorithm from the literature [2] for the particular case, the energy  $E$  of the uncontrolled pendulum must be derived first.

Let us now first consider the equations for the pendulum without the cart. The normalized energy of the pendulum is

$$E = (m_2 L + m_T L_T)g(\cos \varphi - 1) + \frac{J_T}{2} \dot{\varphi}^2 \quad (24)$$

and the control law according to [2] is

$$\ddot{x} = \text{sat}_{ng}(k_1(E - E_0)\text{sign}(\dot{\varphi} \cos \varphi)) \quad (25)$$

where  $\text{sat}_{ng}$  denotes a linear function that saturates at  $ng$ , and  $E_0$  denotes energy desired value. In our case, the control signal is dc-motor voltage and, therefore, we simply apply  $u = \ddot{x}$ . Fig. 3 shows simulation results with energy control algorithm from (25) on the nonlinear model of the pendulum. The parameter  $k_1 = 100$  gives the so-called bang-bang strategy.

The pendulum swings into the upright position in four swings. This gives us a minimal time solution, but the algorithm cannot be applied on the real inverted pendulum because we did not consider a limited length of the cart movement. Even if we start to swing a pendulum from one of the edge position of the pendulum cart on the rail, the cart will reach the second edge of the pendulum rail.

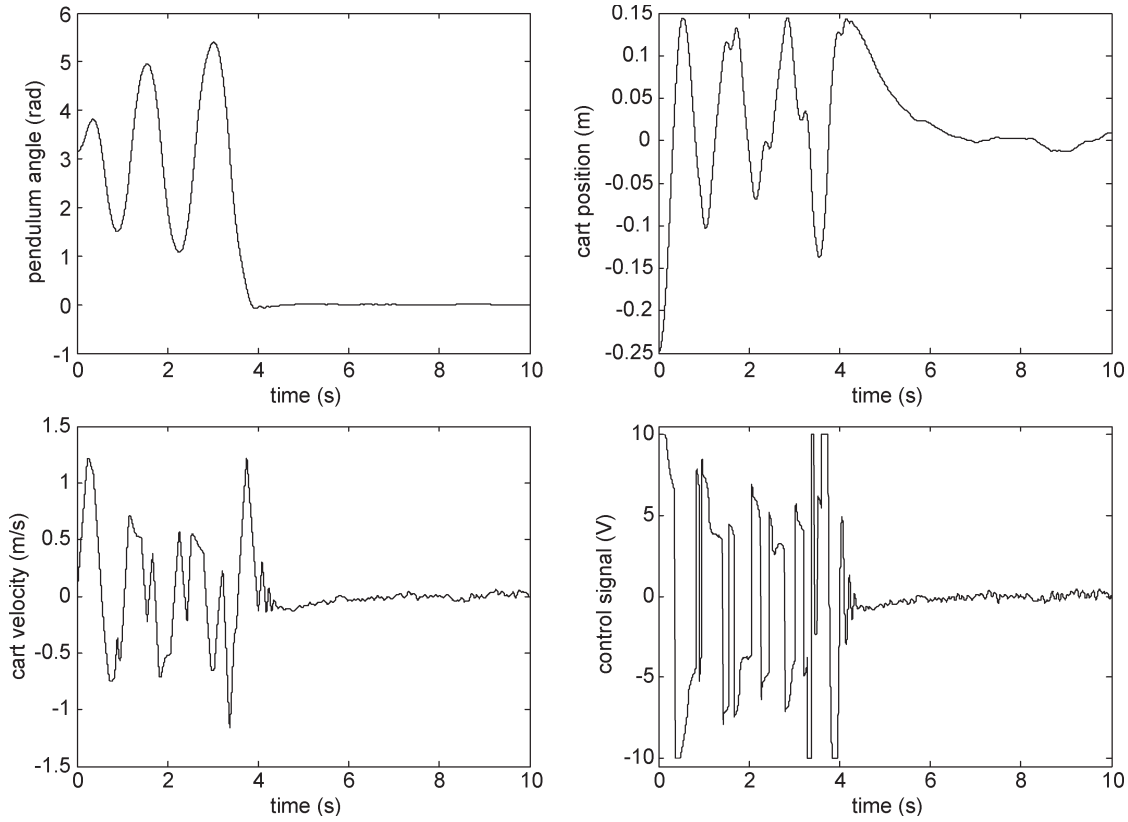


Fig. 4. Swinging up the pendulum with the extended energy control in six swings and stabilization with the state controller:  $k_{su} = 4$ ,  $k_{cw} = 2.25$ ,  $k_{vw} = 0.32$ , and  $k_{em} = 7$ .

Chatterjee *et al.* [11] solves the cart-movement restriction by introducing a cart-potential well, cart-velocity well, and energy maintenance all incorporated in to the control law

$$\begin{aligned} \ddot{x} = & -k_{su}\text{sign}(\dot{\varphi} \cos \varphi) \\ & + k_{cw}\text{sign}(x) \log\left(1 - \frac{|x|}{\left(\frac{x_{\max}}{2}\right)}\right) \\ & + k_{vw}\text{sign}(\dot{x}) \log\left(1 - \frac{|\dot{x}|}{\dot{x}_{\max}}\right) \\ & + k_{em}(\exp |E - E_0| - 1) \text{sign}(E - E_0) \text{sign}(\dot{\varphi} \cos \varphi) \quad (26) \end{aligned}$$

where  $x_{\max} = 0.5$  m is the pendulum-rail length,  $\dot{x}_{\max} = 0.5345$  m/s is the maximum cart velocity that the system is capable of withstanding,  $k_{su}$ ,  $k_{cw}$ ,  $k_{vw}$ , and  $k_{em}$  are the design parameters that need to be adjusted. Fig. 4 shows the simulation results with energy control algorithm from (26) on the nonlinear model of the pendulum.

The pendulum swings into the upright position in six swings and the cart remains within the pendulum-rail limits. The control law from (26) may be implemented on a real inverted pendulum, where all state variables  $\varphi$ ,  $\dot{\varphi}$ ,  $x$ , and  $\dot{x}$  need to be measured and the design parameters  $k_{su}$ ,  $k_{cw}$ ,  $k_{vw}$ , and  $k_{em}$  must be well adjusted. Because in the particular case of the cart inverted-pendulum system, only the cart position  $x$  and the pendulum angle  $\varphi$  are directly measured, the cart velocity  $\dot{x}$  and the angle velocity  $\dot{\varphi}$  must be calculated. Fig. 5 shows the simulation results where two real differentiators with

$100 \text{ s}^{-1}$  cutoff frequency were used for the cart velocity and angle-velocity calculation from the cart-position and pendulum-angle measurements, respectively.

It is obvious that the pendulum could not reach the upright position while the cart remains within the pendulum-rail limits. The real-time implementation of an extended energy controller from (26) needs an exact measurement of all state variables and, therefore, it is unfortunately not applicable on the particular real cart inverted-pendulum system.

### B. Fuzzy Control—Multiswing Behavior

From the basic position after a small impulse, the pendulum should swing up to the upper position without overstepping the limited course of motion. The principle of swinging up is based on the increase of the pendulum energy concerning the pendulum-cart movement limitation.

- 1) For small angles  $|\varphi| < \pi/2$ 
  - a) If the angle  $\varphi$  is positive (negative) and if the angle velocity  $d\varphi/dt$  is positive (negative) then the action value is positive (negative).
  - b) If the angle  $\varphi$  and the angle velocity  $d\varphi/dt$  has different sign then the action value is equal zero.
- 2) For medium angles,  $\pm(\pi/2; 3\pi/4)$  the action value is equal zero.
- 3) For big angles close to the upper position  $\pm(3\pi/4; \pi)$ .
  - a) If the angle velocity  $d\varphi/dt$  is small, and it has the same sign like angle  $\varphi$ , then the energy must be increased like in the case 1.

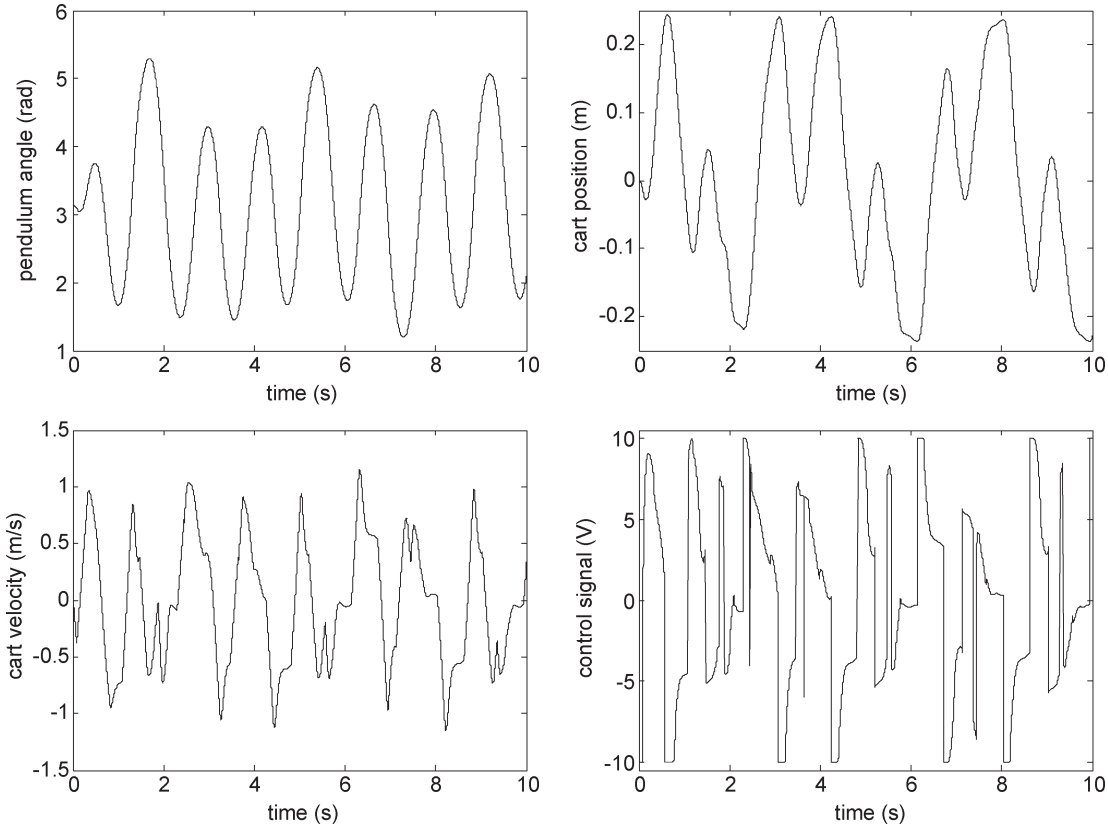


Fig. 5. Swinging up the pendulum with the extended energy controller using real differentiators for cart velocity  $\dot{x}$  and angle velocity  $\dot{\varphi}$  calculation:  $k_{su} = 4$ ,  $k_{cw} = 2.25$ ,  $k_{vw} = 0.32$ , and  $k_{em} = 7$ .

b) If the angle velocity  $d\varphi/dt$  is big, and it has the same sign like the angle  $\varphi$ , then we break the swinging.

4) All these conditions respect that the position of the pendulum cart  $x$  does not overstep the pendulum-rail limits.

The control algorithm was realized with the fuzzy logic system. Three input variables  $\varphi$ ,  $d\varphi/dt$ , and  $x$  and one output variable  $u$  were used. Input variable  $\varphi$  has six membership functions symmetrical by center.

In case 1, we do not need to know the accurate value of the pendulum angle  $\varphi$ , so the rectangular shape of the membership functions has been used. The fuzzy rule base (FRB) consists of 34 rules that well cover proposed fuzzy swing-up strategy. Fig. 6 shows all membership functions.

Definition ranges of variables are cart position:  $x \in [-0.25 \text{ m}, 0.25 \text{ m}]$ , pole angle:  $\varphi \in [-3.14 \text{ rad}, 3.14 \text{ rad}]$ , angle velocity:  $d\varphi/dt \in [-6 \text{ rad/s}, 6 \text{ rad/s}]$ , and dc-motor voltage:  $u \in [-10 \text{ V}, 10 \text{ V}]$ .

A real differentiator with  $100 \text{ s}^{-1}$  cutoff frequency was used for an angle-velocity calculation. Fig. 7 shows the simulation results. The pendulum swings up in five swings. This is a time minimal solution where the pendulum-cart position stays within the pendulum-rail limits and, therefore, this algorithm performs better than the extended energy swinging controller from (26).

The main advantage of using a simple FLC is that it does not need an accurate measurement of all state variables like other model-based methods do and that it is robust on parameter changes and other disturbances in the system. The stability of the proposed FLC strongly depends on the properly designed FRB in the fuzzy swinging algorithm.

## V. BALANCE OF PENDULUM

During the swinging up of the pendulum, a robust state controller may be appropriate to catch the pendulum at the upright position. To switch between swinging and balancing algorithm, the normalized energy of the pendulum  $E$  from (24) is to be calculated and compared with the desired energy of the pendulum  $E_0$ .

The linear-quadratic regulator (LQR) is used for the calculation of the optimal gain matrix  $\mathbf{K}$  such that the state-feedback law

$$u = -\mathbf{K}\mathbf{x} \quad (27)$$

minimizes the cost function

$$J_{\text{LQG}} = \int (\mathbf{x}^T \mathbf{Q} \mathbf{x} + u^T R u) dt \quad (28)$$

subject to the state dynamics

$$\dot{\mathbf{x}} = \mathbf{A}\mathbf{x} + \mathbf{B}u. \quad (29)$$

For the  $\mathbf{Q} = \text{diag}([0.25 \ 0 \ 4 \ 0])$  and  $R = 0.0003$ ; the state-controller vector  $\mathbf{K}$  is

$$\mathbf{K} = [-28.8675 \ -35.1987 \ -137.6009 \ -13.0274]. \quad (30)$$

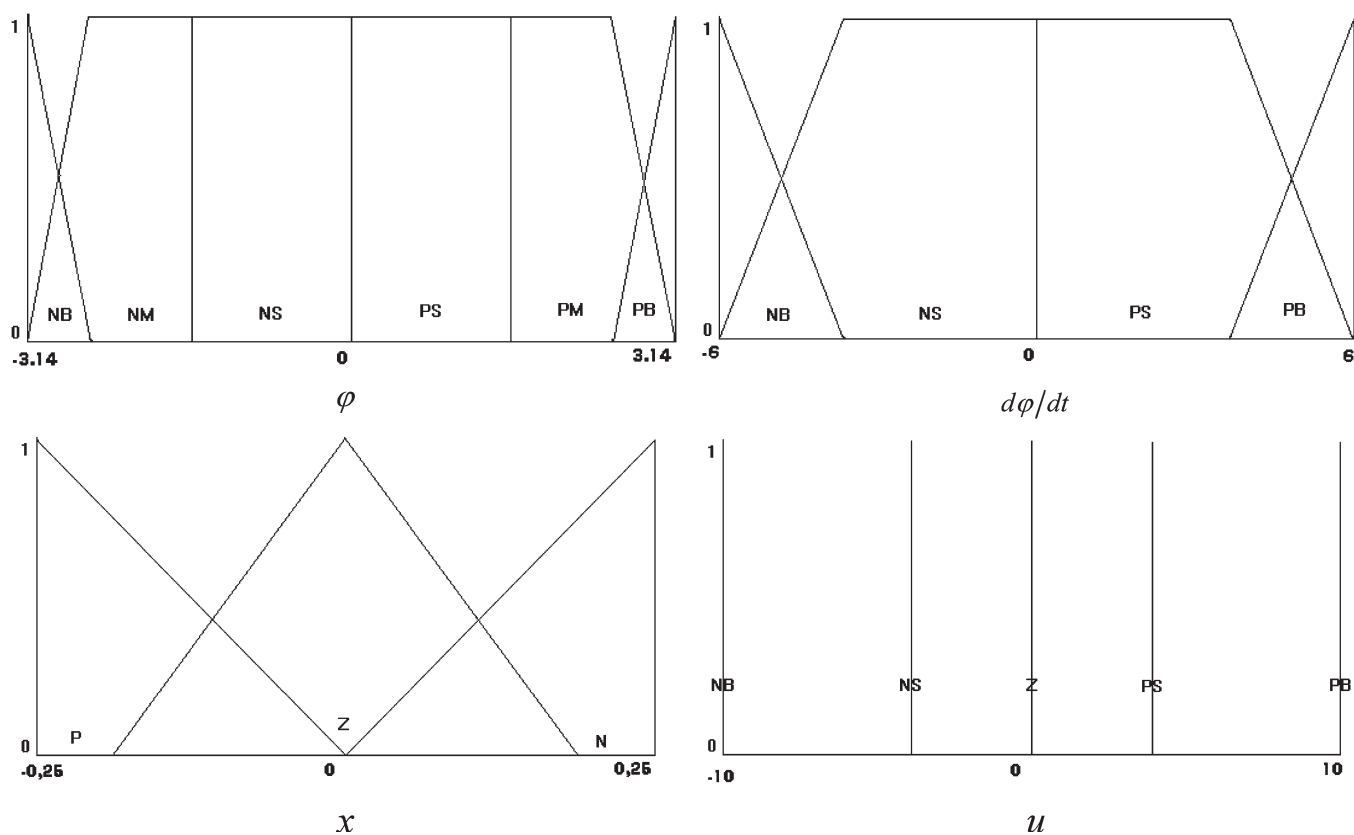


Fig. 6. Membership functions for the fuzzy swinging algorithm.

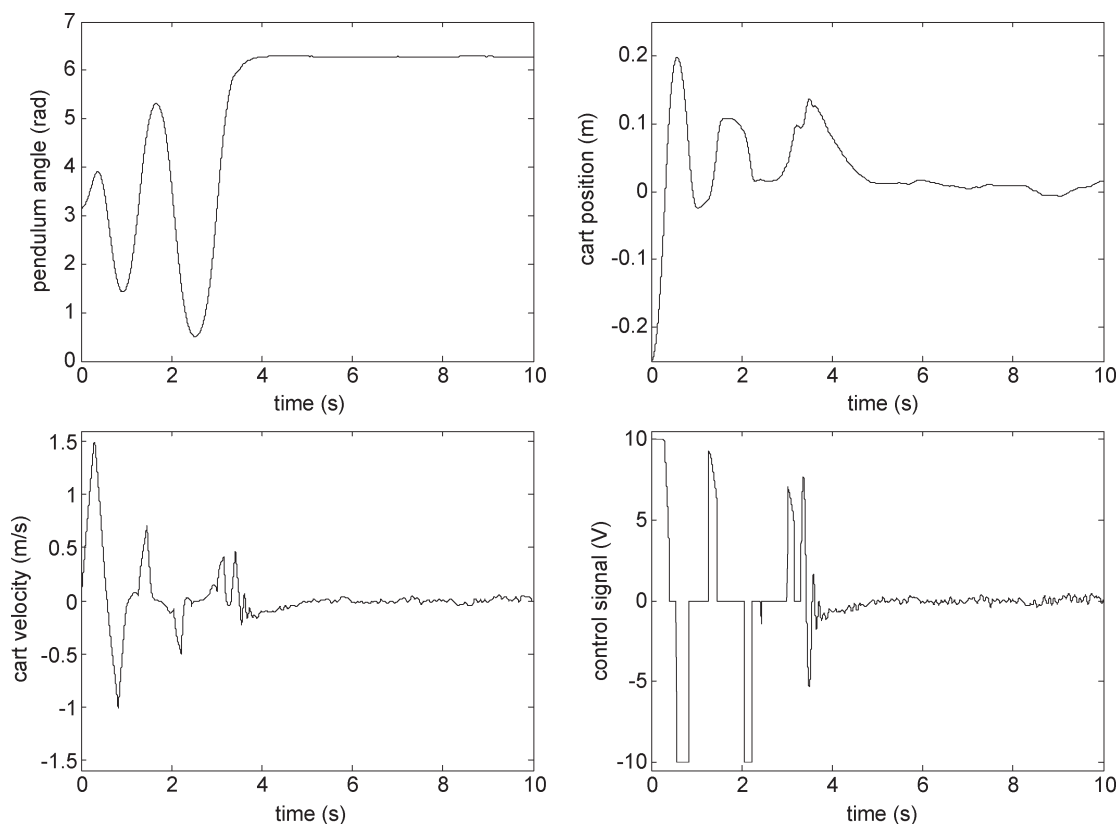


Fig. 7. Swinging up the pendulum with the fuzzy energy control in five swings and stabilization with the state controller.

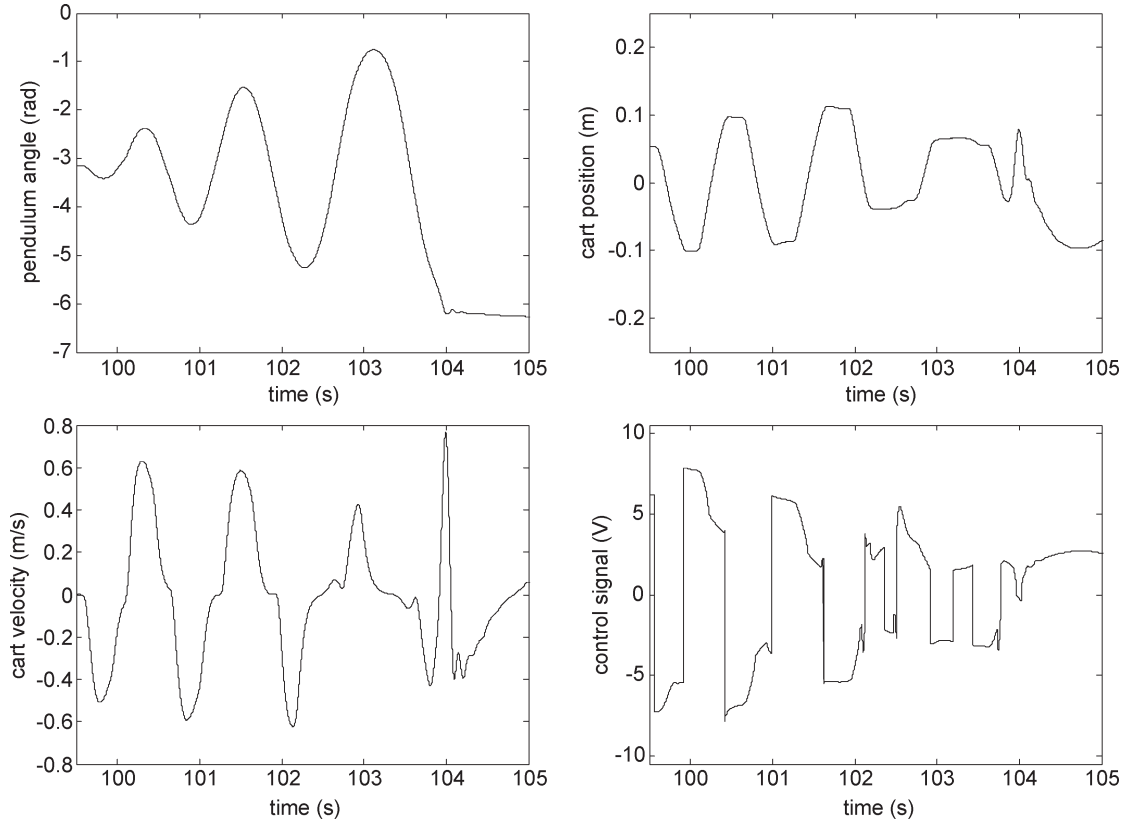


Fig. 8. Swinging up the real pendulum with the fuzzy energy controller and stabilization with the state controller.

The stability of the linearized cart inverted-pendulum model is guaranteed because the LQR design for the proposed state controller is used. This also implies stability of the nonlinear cart inverted-pendulum system near the equilibrium (upright) state where the linear model is evaluated.

#### A. Simulations on Nonlinear Inverted-Pendulum Model

In simulations, the state-controller gain vector  $\mathbf{K}$  from (30) is used to stabilize the nonlinear inverted-pendulum model from (12)–(18), where all pendulum frictions are considered to be negligible  $F_{fr} = M_{fr} = 0$ . Figs. 3, 4, and 7 show that for all swinging algorithms, the state controller is able to stabilize the pendulum at upright position.

#### B. Real-Time Experiment on Real Inverted Pendulum

Fig. 8 shows a real-time experiment on the cart inverted-pendulum system with fuzzy swinging and state-controller balancing algorithm. The pendulum swings into the upright position in two more swings as it does in simulation. This happens because of unconsidered pendulum frictions. The fuzzy swinging algorithm swings the pendulum from any initial condition and the pendulum cart always remain within the pendulum-rail limits. After reaching the upright position, the closed-loop system is stable but the pendulum pole oscillates around the equilibrium point and the cart periodically moves its position. Our aim was to keep the pendulum in/or close to the steady-state position during the activity of defects.

#### C. Adaptive State Controller

While balancing the pendulum in upright position with different state controllers, we recognize that if we want to stabilize the pendulum in to the upper position and to stop any movement of the pendulum cart, we must change the state-controller parameters from robust one to near unstable parameters.

If adaptation method is based on the  $N_2$  norm of the state vector

$$N_2(\mathbf{x}) = \sqrt{\left(\varphi^2 + \left(\frac{d\varphi}{dt}\right)^2 + x^2 + \left(\frac{dx}{dt}\right)^2\right)} \quad (31)$$

then the output of the state controller  $u$  becomes

$$u = k_1 x + (k_2 + N_2(\mathbf{x})) \frac{dx}{dt} + k_3 \varphi + (k_4 - N_2(\mathbf{x})) \frac{d\varphi}{dt} \quad (32)$$

where  $k_1$ ,  $k_2$ ,  $k_3$ , and  $k_4$  are state-controller gains and  $\mathbf{x}$  is a state vector:  $\mathbf{x}^T = [x \ \dot{x} \ \varphi \ \dot{\varphi}]$ .

The adaptive state controller from (32) behaves as a gain-scheduling controller and, therefore, the convergence of the proposed adaptive controller is guaranteed.

Balancing a pendulum with an adaptive state controller after an influence of a disturbance is shown on Fig. 9. The closed-loop control is stable and very impressive. Fig. 10 shows balancing of the pendulum with an adaptive state controller after



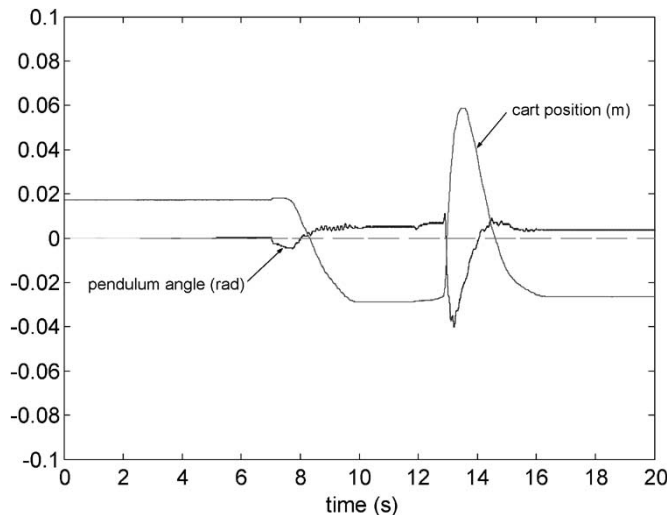


Fig. 9. Balancing the pendulum with the adaptive state controller after disturbance.

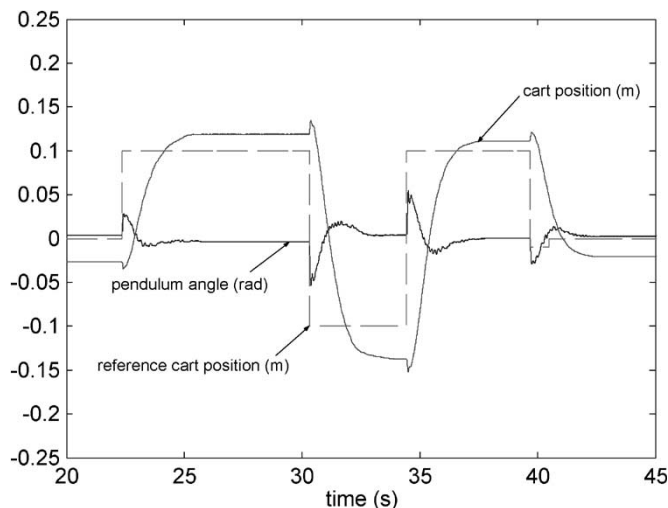


Fig. 10. Balancing the pendulum with the adaptive state controller after changing the reference cart position.

changing the reference cart position. The closed-loop control with an adaptive state controller is stable even after changing the desired cart position and the steady state is reached.

## VI. CONCLUSION

It has been shown that it is very convenient to swing up a pendulum by controlling its energy. The control strategy based on simple fuzzy control algorithm performs even better than the energy controller that was purposed by Åström and Furuta [2] or Chatterjee *et al.* [11]. While swinging up the pendulum, the energy of pendulum is driven toward a value equal to the steady-state upright position, and the pendulum-cart-movement restriction is considered. When the pendulum approaches the upright position, it must be caught with an appropriate strategy. It has been shown that a robust state controller must be designed to capture the pendulum in the upright position. While balancing the pendulum in the upright position with different state

controllers, the pendulum stops at the upper steady state after adapting the state-controller gains. The adaptation method is based on the norm of the state vector. The real-time experiments have been very impressive even during the activity of defects or after changing the desired cart position. The fuzzy swinging algorithm swings the pendulum from any initial condition, and the pendulum cart always remains within the pendulum-rail limits.

## REFERENCES

- [1] K. Furuta, M. Yamakita, and S. Kobayashi, "Swinging up control of inverted pendulum using pseudo-state feed-back," *J. Syst. Control Eng.*, vol. 206, no. 14, pp. 263–269, 1992.
- [2] K. J. Åström and K. Furuta, "Swinging up a pendulum by energy control," *Automatica*, vol. 36, no. 2, pp. 287–295, Feb. 2000.
- [3] J. Yi, N. Yubazaki, and K. Hirota, "Upswing and stabilization of inverted pendulum system based on SIRMs dynamically fuzzy inference model," *Fuzzy Sets Syst.*, vol. 122, no. 1, pp. 139–152, Aug. 2001.
- [4] S. Yurkovich and M. Widjaja, "Fuzzy controller synthesis for an inverted pendulum system," *Control Eng. Pract.*, vol. 4, no. 4, pp. 455–469, Apr. 1996.
- [5] F. H. F. Leung, L. K. Wong, and P. K. S. Tam, "Fuzzy model based controller for an inverted pendulum," *Electron. Lett.*, vol. 32, no. 18, pp. 1683–1685, Aug. 1996.
- [6] H. O. Wang, K. Tanaka, and M. F. Griffin, "An approach to fuzzy control of nonlinear systems: Stability and design issues," *IEEE Trans. Fuzzy Syst.*, vol. 4, no. 1, pp. 14–23, Feb. 1996.
- [7] Q. Wei, W. P. Dayawansa, and W. S. Levine, "Nonlinear controller for an inverted pendulum having restricted travel," *Automatica*, vol. 31, no. 6, pp. 841–850, Jun. 1995.
- [8] C. C. Chung and J. Hauser, "Nonlinear control of a swinging pendulum," *Automatica*, vol. 31, no. 6, pp. 851–862, Jun. 1995.
- [9] C. E. Lin and Y. R. Sheu, "A hybrid control approach for pendulum-cart control," *IEEE Trans. Ind. Electron.*, vol. 39, no. 3, pp. 208–214, Jun. 1992.
- [10] J. Zhao and M. W. Spong, "Hybrid control for global stabilization of the cart-pendulum system," *Automatica*, vol. 37, no. 12, pp. 1941–1951, Dec. 2001.
- [11] D. Chatterjee, A. Patra, and H. K. Joglekar, "Swing-up and stabilization of a cart-pendulum system under restricted cart track length," *Syst. Control. Lett.*, vol. 47, no. 11, pp. 355–364, 2002.



**Nenad Muškinja** (S'91–M'92) received the B.S., M.S., and Ph.D. degrees in electrical engineering from the University of Maribor, Maribor, Slovenia, in 1988, 1992, and 1997, respectively.

Since 1989, he has been a Faculty Member in the Department of Electrical Engineering and Computer Science, University of Maribor, where he currently holds the rank of Assistant Professor. His research interests include industrial automation, adaptive control, sampled-data control, fuzzy control, modeling and process identification, and intelligent systems.



**Boris Tovornik** (M'91) received the B.S. degree from the University of Ljubljana, Ljubljana, Slovenia in 1974 and the M.S. and Ph.D. degrees in electrical engineering from the University of Maribor, Maribor, Slovenia, in 1984 and 1991, respectively.

He is currently an Associate Professor at the University of Maribor. His fields of research interest include computer control of industrial processes, modeling and process identification, fuzzy control, intelligent systems, fault detection, supervision, and safety.